Involvement of oral bacteria-produced short-chain fatty acids in the development of alveolar osteitis

Takayuki Asayama

Nihon University Graduate School of Dentistry,

Major in Oral Surgery

(Directors: Prof. Yoshiyuki Yonehara and

Assoc. Prof. Hiromasa Tsuda)

Contents

This thesis is composed by an article ahead of print and an additional datum listed below.

1. Takayuki Asayama, Ayaka Takada, Yoshikazu Mikami, Hirofumi Yamaguchi, Muneaki Tamura, Kunihito Matsumoto, Kiwa Miyake, Yoshiyuki Yonehara, and Hiromasa Tsuda. Possible roles of short-chain fatty acids produced by oral bacteria in the development of alveolar osteitis. ***J Oral Sci***, ***in press***.

2. RNA-sequencing analysis during RANKL-indued osteoclast formation in the presence or absence of butyrate

Abstract

Alveolar osteitis (dry sockets) is a painful condition characterized by a limited immune response. It is typically caused by the removal of blood clots from extracted tooth sockets, which leads to the fermentation of trapped food remnants by oral bacteria in the cavities, producing high concentrations of short-chain fatty acids (SCFAs). This study examined the effects of SCFAs on immunity and bone metabolism. Mouse macrophage RAW264.7 cells were treated with oral bacterial culture supernatants or SCFA mixtures, and inducible nitric oxide synthase (iNOS) levels were determined by western blot. The same cells were treated with SCFA mixtures in the presence of receptor activator of nuclear factor-κ B ligand (RANKL), and osteoclast-like cells were counted. Newly established clone of MC3T3-E1 cell line (NDC10E1), which can effectively form mineralized nodules, were treated with SCFA mixtures and stained with alizarin red S. On the other hand, genes that were upregulated 4-fold by RANKL treatment and downregulated 4-fold by butyrate treatment on RAW264.7 cells were selected, and gene ontology analysis was performed using the selected genes. RAW264.7 cells treated with oral bacterial culture supernatants of *Porphyromonas gingivalis* and *Fusobacterium nucleatum* inhibited lipopolysaccharide (LPS)-induced iNOS production, likely due to SCFA content. SCFA mixtures mimicking these supernatants almost completely inhibited the number of RANKL-induced tartrate-resistant acid phosphatase positive giant cells and strongly but not completely reduced NDC10E1cell mineralization. On the other hand, SCFA mixtures of *Prevotella intermedia*, *Prevotella nigrescens*, and *Aggregatibacter actinomycetemcomitans* reduced RANKL-induced osteoclastogenesis but not NDC10E1 clone mineralization. Gene ontology analysis indicated that the Rap1 signaling pathway may be involved in the decreased osteoclast formation during RANKL-induced osteoclast formation in the presence of

butyrate. These data suggest that SCFAs produced by *P. gingivalis* and *F. nucleatum* may reduce iNOS production, resulting in reducing inflammatory response. It is also suggested that SCFAs produced by oral bacteria may increase bone mineralization, which thicken the alveolar bone walls via suppressing osteoclastogenesis. These results may contribute to the understanding of alveolar osteitis.

Introduction

Alveolar osteitis, often referred to as dry socket, is a common complication of tooth extraction. When blood clots are removed from the tooth sockets following dental extraction, alveolar osteitis reportedly occurs at an incidence rate of 0.5–5% for routine extractions and more than 30% for mandibular third molar extractions [1,2]. Typical symptoms of this condition include halitosis and intense radiating pain, which is challenging to alleviate with analgesia, in or around the extraction socket. These symptoms cause discomfort in patients after tooth extraction. Although this condition has been known for many years, the etiology of alveolar osteitis is not well understood. During the wound healing process of an extraction socket, blood clots are formed in the cavities, leading to the formation of granulation tissue, which is characterized by the presence of numerous blood capillaries, and subsequent bone formation occurs within the cavities. When the blood clots are completely absent or lysed soon after small clot formation, the underlying cavity bone surfaces are directly exposed to the oral cavities. These conditions result from the activation of plasmin, which lyses fibrin nets in blood clots. This is the widely accepted etiology of alveolar osteitis which is referred to as the fibrinolytic theory [1,3]. As the fibrinolytic activity is also induced by bacterial plasmin activation, poor oral hygiene can be one of the most important risk factors of alveolar

osteitis.

There are several hundred species of microorganisms that inhabit the oral cavity and some of which have inflammatory activators such as lipopolysaccharides (LPS). Although these bacteria can flow into the alveolar cavities, marked signs of inflammation owing to bacterial infection, such as fever and lymphadenopathy, are rarely observed in alveolar osteitis [4-6]. However, the cause of this phenomenon remains unclear. Removing blood clots from the alveolar sockets following tooth extraction creates residences on the socket's surfaces for bacteria to multiply. Impacted food remnants in the cavities are fermented and metabolites are produced by bacteria. Macrophages, patrolling the socket surface encounter these bacterial metabolites. The effect of bacterial culture supernatants from different species on LPS-induced macrophage activation was first investigated in this study. Since the supernatants contain high concentrations of short-chain fatty acids (SCFAs), the effects of SCFAs on LPS-induced macrophage activation, and their influence on receptor activator of nuclear factor-kappa B ligand (RANKL)-induced osteoclast differentiation and osteoblast bone formation were also investigated. The roles of bacterial metabolites for the development of alveolar osteitis after tooth extraction was discussed.

Materials and methods

Reagents

Sodium salts of butyrate, propionate, acetate, formate, and disodium succinate, disodium β-glycerophosphate pentahydrate, and L-ascorbic acid phosphate magnesium salt n-hydrate were purchased from Fujifilm Wako (Osaka, Japan). Sodium isobutyrate and sodium isovalerate were purchased from Kanto Chemical (Tokyo, Japan) and sodium lactate was from Sigma Aldrich (St. Louis, MO, USA).

Oral bacteria used in this study, culture condition, and bacterial cellular supernatant preparations

Oral bacteria including *Porphyromonas gingivalis* (*P. gingivalis*) strains W83 and FDC381, *Fusobacterium nucleatum* (*F. nucleatum*) strains ATCC25586 and JCM6328, *Prevotella intermedia* (*P. intermedia*) strain ATCC25611, *Prevotella nigrescens* (*P. nigrescens*) strain ATCC33563, and *Aggregatibacter actinomycetemcomitans* (*A. actinomycetemcomitans*) strain Y4 were anaerobically cultured in brain heart infusion (BHI) broth (BD, Franklin Lakes, NJ, USA) supplemented with 5 ppm hemin and 0.5 ppm menadione at 37°C, and cell culture supernatants were collected by centrifugation at 10,000 × *g* for 20 min at 4°C to remove bacterial cells and sterilized using 0.22-μm pore size filter units. One tenth of the bacterial culture supernatants were diluted in mammalian

cell culture medium.

SCFA quantitation in bacterial culture supernatants and preparation of SCFA mixtures which mimics bacterial supernatants

SCFA concentrations in the supernatants were determined using gas chromatography as previously described [7]. Briefly, phosphoric acid-acidified bacterial culture supernatants were mixed with two times volume of acetonitrile. After protein or peptide precipitation by centrifugation, the supernatants were applied to a GC-2010 capillary gas chromatograph (Shimadzu, Kyoto, Japan) with a free fatty acid phase capillary column. SCFA-mixtures, designed to mimic the composition found in bacterial cell culture supernatants, were prepared based on the SCFA concentrations observed in each bacterial culture supernatant.

Cell culture

Mouse macrophage RAW264.7 cells were purchased from Dainippon Pharmaceutical (Osaka, Japan). MC3T3-E1 cells were provided by the Riken BioResourse Research Center (Tsukuba, Japan). Both cell lines were maintained in 10% fetal bovine serum (FBS, Cytiva, Marlborough, MA, USA) containing minimum essential medium α (MEMα, Fujifilm Wako) supplemented with penicillin and streptomycin (Fujifilm Wako) at 37°C. For mineralization experiments, 10%FBS MEMα containing 10 mM disodium β-

glycerophosphate pentahydrate and 50 μg/ml L-ascorbic acid phosphate magnesium salt n-hydrate was used as a mineralization medium.

Western blot

RAW264.7 cells (4×10^6 cells/well) were plated onto a 24-well cell culture plate. Cells were treated for 8 h with bacterial culture supernatants (1/10 volume), sodium butyrate (5 or 10 mM), sodium propionate (10 or 20 mM), sodium isobutyrate (10 or 20 mM), sodium isovalerate (10 or 20 mM), sodium acetate (10 or 20 mM), sodium lactate (10 or 20 mM), sodium formate (10 or 20 mM), disodium succinate (10 or 20 mM), or mimics of bacterial culture supernatants. Equal amounts of total protein from cell lysates were applied to sodium dodecyl sulfate-polyacrylamide gel electrophoresis (5-20% polyacrylamide gradient gel), and the separated proteins were transferred onto a polyvinylidene difluoride membrane. The membrane was treated for 30 min with an Ez-Block Chemi blocking reagent (ATTO, Tokyo, Japan). An anti-inducible nitric oxide synthase (iNOS) polyclonal antibody (GeneTex, Irvine, CA, USA) and WestVision Peroxidase Polymer, anti-rabbit IgG (Vector Laboratories, Newark, CA, USA) were used as primary and secondary antibodies, respectively. An anti-glyceraldehyde-3-phosphate dehydrogenase (GAPDH) mouse IgG (Santa Cruz Biotechnology, Dallas, TX, USA) and WestVision Peroxidase Polymer, anti-mouse IgG (Vector Laboratories) were used for

internal control detection. The band images were developed using a Clarity Western ECL reagent (BIO-RAD, Hercules, CA, USA) and photographed using a ChemiDoc XRS system (BIO-RAD).

Osteoclast-like cell differentiation

RAW264.7 cells (3×10^3 cells/well) were plated on a 48-well plate and incubated overnight at 37°C. Media were changed to 10%FBS MEMα containing sodium butyrate (1 mM), sodium propionate (5 mM), sodium isobutyrate (10 mM), sodium isovalerate (10 mM), sodium acetate (10 mM), sodium lactate (10 mM), sodium formate (10 mM), disodium succinate (10 mM), or SCFA mixtures that mimic bacterial culture supernatants. Recombinant mouse RANKL (PeproTech, Cranbury, NJ, USA) at a concentration of 50 ng/ml was added, and cells were cultured for 4 days. Cells were fixed by 10% formaldehyde (Fujifilm Wako), treated with 0.1% Triton X-100, and stained with tartrate-resistant acid phosphatase (TRAP) staining solution. The plates were scanned with a GT-X830 flat-head scanner (Seiko Epson, Suwa, Japan). TRAP-positive cells that have more than three nuclei were counted as osteoclast-like cells.

Mineralization assay

A murine osteoblast-like MC3T3-E1 line is a group of cells with heterogeneous characteristics [8]. Thus, using a limited dilution method, a clonal line was established

and named clone NDC10E1, which can effectively form mineralized nodules. The clone forms mineralized tissue within 7 days in the mineralization medium and was used as preosteoblastic cells in this study. NDC10E1 cells (2×10^5 cells/well) were plated on a 24-well plate and incubated overnight at 37°C (this condition can allow the cells to reach confluence in the next day). Media were changed to a mineralization medium in the presence or absence of each SCFA or mimics of bacterial culture supernatants and cells were incubated for 6 days at 37°C. Media were changed every 2 or 3 days. Alizarin red S staining was performed to evaluate mineralization. The stained plates were scanned using a GT-X830 (Seiko Epson) and mean intensities of each well were measured using a Fiji/ImageJ software [9].

RNA-sequencing analysis

RAW264.7 cells (1.7×10^5 cells) were seeded in a 10 cm tissue culture dish and incubated overnight at 37°C. The cultures were then treated for 48 h with 50 ng/ml of recombinant mouse RANKL in the presence or absence of 1 mM butyrate in 10% FBS MEMα. An untreated culture was prepared as a control. Total RNA was extracted and purified using ISOGEN with a Spin Column Kit (NIPPON GENE, Tokyo, Japan). RNA concentration and quality were assessed using NanoDrop (Thermo Fisher) and Bioanalyzer (Agilent Technologies, Santa Clara, CA, USA). For RNA-sequencing analysis, RNA libraries were

prepared using the SMART-Seq v4 ultra low input RNA kit for sequencing (Clontech, Mountain View, CA, USA) and the Nextera XT DNA library prep kit (Illumina, San Diego, CA, USA). Paired-end sequencing was performed (150 bp × 2, 66 M reads, and 6 GB data/sample) using a NovaSeq 6000 sequence system (Illumina) with a NovaSeq 6000 [S4/SP] reagent kit (Illumina) and NovaSeq [Xp 4-Lane/Xp 2-Lane] kit (Illumina). Sequence quality was checked using the NovaSeq control software (ver. 1.7.5, Illumina). Sequence trimming, mapping of read sequences, read counts, and transcripts per million (TPM) calculations were performed using DRAGEN Bio-IT platform (ver. 3.9.3, Illumina). The cutoff value for TPM was < 0.01. Genes that were upregulated more than four times by RANKL treatment compared to untreated control and those that were downregulated by less than a quarter in the presence of butyrate compared to RANKL treatment in the absence of butyrate were extracted. Calculation and Venn diagram drawing were performed using Microsoft Excel (Microsoft, Redmond, WA, USA). A database for annotation, visualization, and integrated discovery program (DAVID, National Institute of Health) was used for gene ontology (GO) enrichment analysis.

Statistical analysis

Statistical analyses were conducted using the EZR program (Saitama Medical Center, Jichi Medical University, Saitama, Japan [10]. The Shapiro-Wilk normality test was

employed to assess the distribution of the data, which revealed a non-normal distribution. Consequently, the Kruskal-Wallis test, followed by the Steel test, was used to evaluate the differences. Results yielding a *P*-value of less than 0.05 were interpreted as statistically significant.

Results

SCFAs produced by *P. gingivalis* and *F. nucleatum* suppress LPS-induced iNOS production on RAW264.7 cells.

To examine the effects of oral bacterial metabolites on LPS-induced macrophage activation, RAW264.7 cells were treated with culture supernatants of oral bacteria. Although LPS (100 ng/ml) treatment with RAW264.7 cells induced iNOS production, treatments with bacterial culture supernatants of *P. gingivalis* or *F. nucleatum* strongly suppressed LPS-induced iNOS production (Fig. 1A). In contrast, supernatants from *P. intermedia*, *P. nigrescens*, and *A. actinomycetemcomitans* did not strongly suppress LPS-induced iNOS levels. As oral bacteria ferment dietary fibers and produce high concentrations (mM-order) of several types of SCFAs [11], the concentration of each SCFA in the bacterial culture supernatants was examined using gas chromatography (Table 1). Relatively high concentrations of butyrate (19.095-32.414 mM), propionate (5.576-9.065 mM), and isobutyrate (8.156-19.991 mM) were found in culture supernatants of *P. gingivalis* and *F. nucleatum* of which culture supernatants strongly suppressed LPS-induced iNOS production (Table 1 and Fig. 1A). Next, the effects of each SCFAs contained in bacterial culture supernatants on LPS-induced M1 macrophage activation were examined. Treatment of RAW264.7 macrophage cells with butyrate,

propionate, isobutyrate, and isovalerate strongly suppressed LPS-induced iNOS production (Fig. 1B). Although acetate treatment slightly repressed LPS-induced iNOS production, other SCFA (lactate, formate, succinate) treatments did not reduce LPS-induced iNOS production (Fig. 1B). SCFA mixtures mimicking the respective bacterial culture supernatants were subsequently prepared and the effects of these mixtures on LPS-induced iNOS production were examined. Only SCFA mixtures that mimic *P. gingivalis* and *F. nucleatum* culture supernatant reduced LPS-induced iNOS production (Fig. 1C). These results demonstrated that SCFAs which are produced by *P. gingivalis* and *F. nucleatum* suppress LPS-induced macrophage activation. Especially, butyrate, propionate, isobutyrate, and isovalerate have potent effects on this phenomenon.

SCFAs produced by oral bacteria inhibit RANKL-induced osteoclast formation.

The effects of SCFAs produced by oral bacteria on bone metabolisms were subsequently examined. As shown in Fig. 2A, treatment with butyrate, propionate, isobutyrate, and isovalerate almost completely inhibited RANKL-induced TRAP-positive multinuclear cell formation. Although acetate, lactate, and succinate treatment significantly reduced RANKL-induced TRAP-positive multinuclear cell formation, more than 50 TRAP-positive cells were still observed (Fig. 2A). Although treatment with SCFA mixtures which mimic *P. gingivalis* or *F. nucleatum* culture supernatants almost completely

suppressed RANKL-induced TRAP-positive multinuclear cell formation (Fig. 2B), treatment with SCFA mixtures which mimic culture supernatants of *P. intermedia*, *P. nigrescens*, and *A. actinomycetemcomitans* significantly reduced RANKL-induced TRAP-positive cell formation (Fig. 2B). However, the reduced rates are weaker than those of *P. gingivalis* and *F. nucleatum* (Fig. 2B).

Treatment with butyrate, propionate, isobutyrate, and isovalerate reduces mineralization by osteoblast-like NDC10E1 cells.

To investigate the effect of SCFA treatment on the osteogenic function of osteoblasts, murine osteoblast-like NDC10E1cells were treated with each SCFA and mineralization abilities were evaluated using alizarin red S staining. While treatment of NDC10E1cells with butyrate, propionate, isobutyrate, isovalerate, and succinate reduced mineralization induced by the mineralization medium (Fig. 3A), treatment with acetate, lactate, or formate did not alter the mineralization of NDC10E1cells in the presence of a mineralization medium (Fig. 3A). Next, the effects of SCFA-mixtures that mimic oral-bacterial culture supernatants were examined. Mineralization levels of cells treated with SCFA mixtures mimicking *P. gingivalis* strains W83, FDC381, *F. nucleatum* strains ATCC25586, and JCM6328 in the presence of a mineralization medium were 11.4, 38.1, 45.8, and 53.2% lower, respectively, when compared to untreated cells (Fig. 3B).

Treatment with SCFA mixture mimicking other bacterial culture supernatants (*P. intermedia*, *P. nigrescens*, and *A. actinomycetemcomitans*) did not alter mineralization level (Fig. 3B).

Transcriptome analysis

SCFAs produced by oral bacteria reduced the formation of osteoclast-like cells as described above. Whole transcript expressions using high throughput sequencing technology was examined to extract candidate genes related to inhibitory effects of butyrate treatment on RANKL-induced osteoclast formation. RANKL-treatment upregulated 1,281 genes with expression levels more than four times compared to those of the untreated control (Fig. 4). Of which 595 genes were downregulated by a quarter time on butyrate treatment compared to those of butyrate treatment in the presence of RANKL (Fig. 4). Among 595 genes, the top 20 genes that were upregulated by RANKL treatment are listed in Table 2. Although several genes related to membrane and cytoskeletal modification were identified such as *Sphk1*, *Sgms2*, and *Cttn*, genes related to osteoclast differentiation were not found in the list (Table 2). Among 595 genes, 566 genes with Entrez gene IDs were further used for Kyoto Encyclopedia of Genes and Genomes (KEGG) pathway GO enrichment analysis using the DAVID program; the top 10 related KEGG pathways are listed in Table 3. The highest ranked pathway, which is

associated with osteoclast differentiation, was the Rap1 pathway [12,13]. Active Rap1 induces osteoclast differentiation [14]. Six genes (highlighted with stars in Fig. 5) whose products activate Rap1 were included in 566 gene (Fig. 5). Therefore, enriched gene products may induce Rap1 activation and subsequent osteoclastogenesis.

Discussion

It was demonstrated that treatment of macrophage-like RAW264.7 cells with bacterial culture supernatants from *P. gingivalis* and *F. nucleatum*, in which contain high concentrations of butyrate, propionate, isobutyrate, and isovalerate, suppressed LPS-induced iNOS production (Fig. 1A, B, and C). These data suggested that bacteria-producing SCFAs, particularly butyrate, propionate, isobutyrate, and isobutyrate, have reducing effects on LPS-induced M1-like macrophage activation. Macrophages are functionally divided into two types. M1-type macrophages activated by LPS and interferon (IFN)-γ strongly produce inflammatory cytokines such as tumor necrosis factor (TNF)-α, IL-1, and IL-6, resulting in the activation of inflammation, immune response, and subsequent pathogen killing [15,16]. The induction of iNOS is a marker for macrophages of the M1 type. [15,16]. M2-type macrophages downregulate the production of inflammatory cytokines and upregulate anti-inflammatory cytokines, resulting in inhibition of inflammation and subsequent tissue restoration [16]. Removal of the blood clot exposes the extracted cavities to oral bacteria, allowing for the easy flow of bacteria into the cavities. Since oral bacteria in the cavities metabolize residual food remnants and produces high concentrations of SCFAs [11], the data presented suggest that SCFAs produced by *P. gingivalis* and *F. nucleatum* may suppress the activation of

M1-type macrophages, thereby reducing inflammation. SCFAs produced by oral bacteria such as butyrate, propionate, isobutyrate, and isovalerate may have strong effects to suppress the inflammation and subsequent immune response. Since Letvin et al.'s study suggests that there is a relationship between alveolar osteitis and immune-compromised patients [17], the immune response suppressed by bacteria-derived SCFAs may play an important role in the development of alveolar osteitis.

SCFAs produced by oral bacteria can affect the bone surface of sockets that do not have a blood clot. SCFA mixtures that mimic culture supernatants of *P. gingivalis* and *F. nucleatum* almost completely suppressed RANKL-induced osteoclast-like cell formation (Fig. 2B). These culture supernatants contain high or relatively high concentrations of butyrate, propionate, isobutyrate, and isovalerate, which almost completely suppressed RANKL-induced osteoclast formation (Table 1, Fig. 2A). Mimic of bacterial culture supernatants of *P. gingivalis* strain FDC381 and *F. nucleatum* strongly, but not completely, reduced mineralization (Fig. 3B). These data suggest that treatment of the bone surface with SCFAs in culture supernatants of *P. gingivalis* strain FDC381 and *F. nucleatum* may induce a gradual increase of bone mineralization. The culture supernatant mimic of *P. gingivalis* strain W83 almost completely reduced RANKL-induced osteoclastgenesis but resulted in only a small decrease in mineralization by

osteoblasts. This SCFA mixture may exhibit much stronger bone mineralization compared to those of *P. gingivalis* strain FDC381 and *F. nucleatum*. By contrast, treatment with SCFA mixtures of *P. intermedia*, *P. nigrescens,* and *A. actinomycetemcomitans* significantly reduced the number of TRAP-positive multinuclear giant cells (but many TRAP-positive small cells remained) and maintained ordinary levels of mineralization by osteoblasts. Although this condition may induce bone mineral content, it depends on the bone resorptive abilities of the single nuclear cells. The effects of oral bacterial products on bone metabolism seems to be dependent on SCFA ingredients produced by oral bacteria.

GO pathway analysis was performed using whole transcriptomes and the top 10 enriched pathways are listed in Table 3. The highest-ranked pathway related to osteoclast differentiation was the Rap1 signaling pathway (Table 3). As presented in Figure 5, diverse receptor signals such as calmodulin signaling, G-protein coupled receptor signaling, and growth factor signaling, change Rap1 from a GDP-binding inactive status to a GTP-binding active status. Active Rap1 promotes the association of Talin1 with the cytoplasmic domain of integrin, leading to a high-affinity conformation [14]. This conformational change results in the activation of Rac1 through the complex of c-Src, Syk, Dap12, and VAV3, which induces RANKL-mediated osteoclast formation [14].

Activated Rac1 induces RANKL-induced osteoclastogenesis through nuclear factor-κB activation [12]. Therefore, the inhibitory effects of butyrate on RANKL-induced osteoclastogenesis may be mediated via Rap1 signaling. Further studies are required to elucidate the mechanisms underlying the effects of SCFAs.

It can be concluded that SCFAs produced by *P. gingivalis* and *F. nucleatum* can inhibit endotoxin-induced inflammation in the tooth sockets when the blood clot drops off from the cavities after extraction. Since frank signs of infectious inflammation such as fever, leukocytosis, and lymphadenopathy are rare in alveolar osteitis patients [18], inhibitory effects of the SCFAs on LPS-induced M1 macrophage activation may be corresponding to the symptoms of alveolar osteitis. However, the name "alveolar osteitis" may not match with its pathological condition. *P. gingivalis* and *F. nucleatum*-producing SCFAs may add mineralized tissue on the alveolar bone walls of the socket. The increased cavity bone wall thickness due to SCFA effect may decrease blood supplies to the cavities, leading to a decrease in immune cell migration to the cavities. This condition may lead to the survival of bacteria in the cavity, causing poor oral hygiene and halitosis. Since these findings align with the physical observation of alveolar osteitis, SCFAs produced by oral bacteria in the tooth extraction cavities after the loss of blood clots might have the potential to contribute to the development of some of the symptoms of alveolar osteitis.

Further studies are needed for understanding the relationship between SCFAs and alveolar osteitis.

Taken together, SCFAs produced by oral bacteria especially by *P. gingivalis* and *F. nucleatum* may inhibit the immune response and mildly add mineralization of the alveolar bone walls during alveolar osteitis development.

Acknowledgments

The author expresses its sincere thanks to Prof. Yonehara of the Department of Oral and Maxillofacial Surgery II, Nihon University School of Dentistry, for his sophisticated tutelage. The author is grateful to Assoc, Prof. Tsuda, Department of Biochemistry, Nihon University School of Dentistry, for his enthusiastic mentorship and assistance. The author thanks Dr. Mikami (Division of Microscopic Anatomy, Niigata University Graduate School of Medical and Dental Sciences), Dr. Matsumoto (Department of Oral and Maxillofacial Radiology, Nihon University School of Dentistry), and Dr. Miyake (Division of Oral Structural and Functional Biology, Nihon University Graduate School of Dentistry) for their helpful suggestions and discussions. The author would like to thank to Dr. Takada (Nihon University School of Dentistry) and Dr. Yamaguchi (Nihon University School of Dentistry) for their friendship as a colleague.

References

1. Chow O, Wang R, Ku D, Huang W (2020) Alveolar osteitis: a review of current concepts. J Oral Maxillofac Surg 78, 1288-1296.

2. Ghosh A, Aggarwal VR, Moore R (2022) Aetiology, prevention and management of alveolar osteitis-a scoping review. J Oral Rehabil 49, 103-113.

3. Blum IR (2002) Contemporary views on dry socket (alveolar osteitis): a clinical appraisal of standardization, aetiopathogenesis and management: a critical review. Int J Oral Maxillofac Surg 31, 309-317.

4. Nitzan DW (1983) On the genesis of "dry socket". J Oral Maxillofac Surg 41, 706-710.

5. Amaratunga NA, Senaratne CM (1988) A clinical study of dry socket in Sri Lanka. Br J Oral Maxillofac Surg 26, 410-418.

6. Krakowiak PA (2011) Alveolar osteitis and osteomyelitis of the jaws. Oral Maxillofac Surg Clin North Am 23, 401-413.

7. Imai K, Ochiai K, Okamoto T (2009) Reactivation of latent HIV-1 infection by the periodontopathic bacterium *Porphyromonas gingivalis* involves histone modification. J Immunol 182, 3688-3695.

8. Wang D, Christensen K, Chawla K, Xiao G, Krebsbach PH, Franceschi RT (1999)

Isolation and characterization of MC3T3-E1 preosteoblast subclones with distinct in vitro and in vivo differentiation/mineralization potential. J Bone Miner Res 14, 893-903.

9. Schindelin J, Arganda-Carreras I, Frise E, Kaynig V, Longair M, Pietzsch T, Preibisch S, Rueden C, Saalfeld S, Schmid B, Tinexez JY, White DJ, Hartenstein V, Eliceiri K, Tomancak P, Cardona A. (2012) Fiji: an open-source platform for biological-image analysis. Nat Methods, 9, 676–682.

10. Kanda Y (2013) Investigation of the freely available easy-to-use software 'EZR' for medical statistics. Bone Marrow Transplant 48, 452-458.

11. Pöllänen MT, Salonen JI, Uitto VJ (2003) Structure and function of the tooth-epithelial interface in health and disease. Periodontol 2000 31, 12-31.

12. Lee NK, Choi HK, Kim DK, Lee SY (2006) Rac1 GTPase regulates osteoclast differentiation through TRANCE-induced NF-κB activation. Mol Cell Biochem 281, 55-61.

13. Wang Y, Lebowitz D, Sun C, Thang H, Grynpas MD, Glogauer M (2008) Identifying the relative contributions of Rac1 and Rac2 to osteoclastogenesis. J Bone Miner Res 23, 260-270.

14. Zou W, Izawa T, Zhu T, Chappel J, Otero K, Monkley SJ, Critchley DR, Petrich

BG, Morozv A, Ginsberg MH, Teitelbaum SL. (2013) Talin1 and Rap1 are critical for osteoclast function. Mol Cell Biol 33, 830-844.

15. Biswas SK, Mantovani A (2010) Macrophage plasticity and interaction with lymphocyte subsets: cancer as a paradigm. Nat Immunol 11, 889-896.

16. Gordon S, Martinez FO (2010) Alternative activation of macrophages: mechanism and functions. Immunity 32, 593-604.

17. Levitin SA, Jeong IC, Finkelstein J (2019) Mining electronic dental records to identify dry socket risk factors. Stud Health Technol Inform 262, 328-331.

18. Rohe C, Schlam M (2023) Alveolar osteitis. In StatPearls, StatPearles Publishing, https://www.ncbi.nlm.nih.gov/books/NBK430685/

Table 1. SCFA concentrations in supernatant of bacterial cultures

Bacterial strains	SCFA (mM)							
	Butyrate	Propio-nate	Iso-butyrate	Iso-valerate	Acetate	Formate	Lactate	Succinate
BHI broth containing hemine and menadione	0.000	3.637	4.837	0.000	2.875	0.284	0.532	0.233
Porphyromonas gingivalis								
W83	19.095	6.719	19.991	8.067	10.961	0.329	0.000	0.202
FDC381	24.386	9.065	15.841	13.159	11.802	0.641	0.000	0.963
Fusobacterium nucleatum								
ATCC25586	32.414	7.365	8.219	0.000	11.452	8.824	0.000	0.202
JCM6328	31.622	5.576	8.156	0.000	10.976	8.781	0.000	0.224
Prevotella intermedia								
ATCC25611	0.000	3.729	0.000	1.755	24.065	15.680	0.000	6.996
Prevotella nigrescens								
ATCC33563	0.000	3.464	0.000	2.737	17.183	8.337	0.000	8.675
Aggregatibacter actinomycetemcomitans								
Y4	0.000	3.446	0.000	0.000	15.598	2.960	9.789	2.894

Table 2. Genes affected by RANKL and butyrate treatment

Ranking	Gene symbol	$\log_2$(RANKL)/(Cont)	$\log_2$(RANKL + Buty) - $\log_2$(RANKL)	Description
1	*Gm21748*	13.92	-13.92	predicted gene, 21748
2	*Gng8*	12.49	-2.042	guanine nucleotide binding protein (G protein), gamma 8
3	*Cfap45*	12.41	-3.689	cilia and flagella associated protein 45
4	*Sphk1*	12.39	-2.443	sphingosine kinase 1
5	*Snapc1l*	11.41	-11.41	small nuclear RNA activating complex, polypeptide 1like
6	*Lce1g*	11.41	-3.569	late cornified envelope 1G
7	*Upp1*	11.26	-3.633	uridine phosphorylase 1
8	*Enpp2*	11.14	-2.187	ectonucleotide pyrophosphatase/phosphodiesterase 2
9	*Gm17606*	10.97	-10.97	predicted gene, 17606
10	*Adig*	10.91	-10.91	adipogenin
11	*Cysrt1*	10.79	-2.010	cysteine rich tail 1
12	*Sprr2k*	10.74	-2.215	small proline-rich protein 2K
13	*Sgms2*	10.72	-5.909	sphingomyelin synthase 2
14	*Tmc4*	10.45	-2.620	transmembrane channel-like gene family 4
15	*Lypd2*	10.40	-10.40	Ly6/Plaur domain containing 2
16	*Mgp*	10.37	-3.357	matrix Gla protein
17	*Bpi*	10.22	-4.366	bactericidal permeablility increasing protein
18	*Eif1ad16*	10.21	-10.21	eukaryotic translation initiation factor 1A domain containing 16
19	*Cttn*	10.04	-10.04	cortactin
20	*Vsig8*	9.910	-2.956	V-set and immunoglobulin domain containing 8

Table 3. Enriched pathways by DAVID gene ontology analysis

Ranking	Terms	Count	%	*P*-value
1	Axon guidance	12	2.1	0.003
2	Rap1 signaling pathway	12	2.1	0.011
3	Adrenergic signal in cardiomyocytes	9	1.6	0.029
4	Aldosterone synthesis and secretion	7	1.2	0.031
5	Calcium signaling pathway	12	2.1	0.034
6	Regulation of action cytoskeleton	11	1.9	0.043
7	PI3E-Akt signaling pathway	15	2.7	0.044
8	Ras signaling pathway	11	1.9	0.047
9	Pancreatic synapse	7	1.2	0.049
10	Glutamatergic synapse	7	1.2	0.049

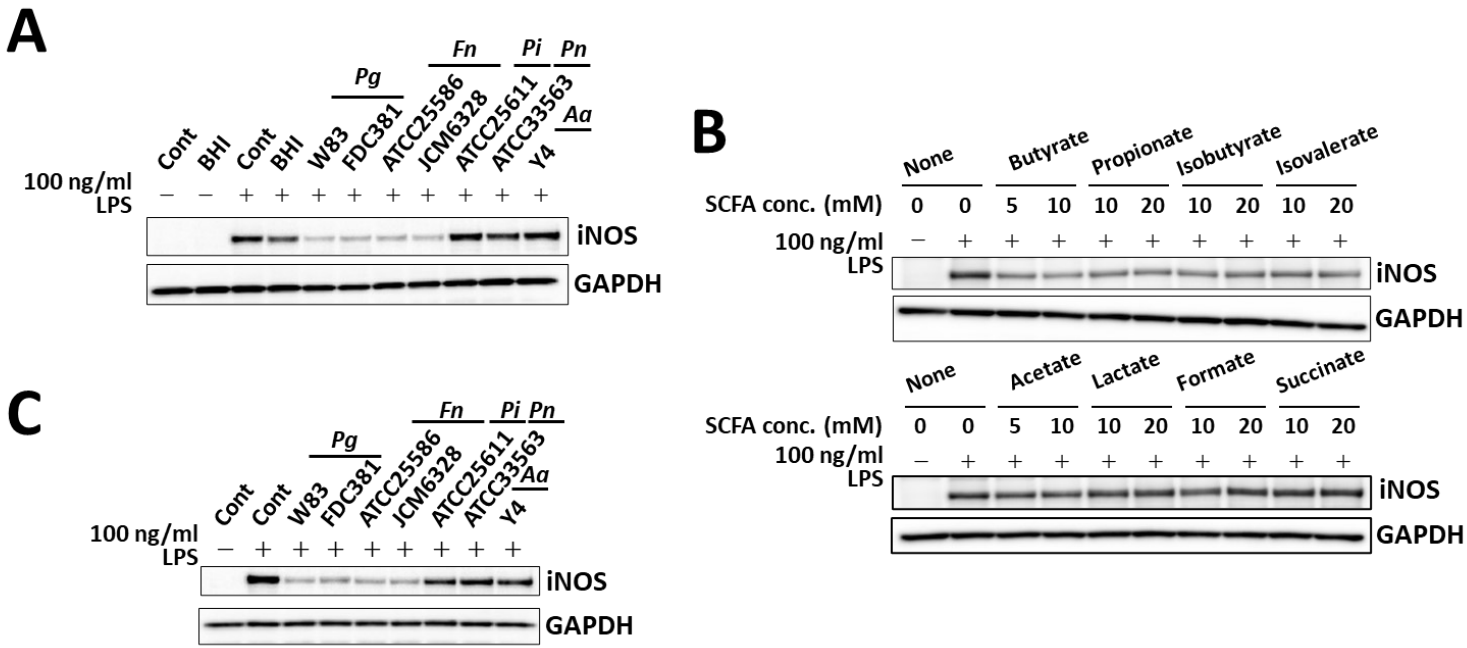

Fig. 1. SCFAs produced by oral bacteria strongly suppress LPS-induced iNOS production.

(A) Murine macrophage RAW264.7 cells were treated for 8 h with 100 ng/ml LPS in the presence or absence of several kinds of bacterial culture supernatants, and cell lysates were subjected to western blot to determine iNOS-levels. GAPDH were used for an internal control. (B) RAW264.7 cells were treated for 8 h with 100 ng/mL LPS in the presence or absence of the indicated concentrations of each SCFAs, and iNOS-levels were examined by western blot. (C) RAW264.7 cells were treated for 8 h with 100 ng/ml LPS in the presence or absence of SCFA-mixtures which mimic bacterial culture supernatants, and iNOS-levels were determined by western blot. *Pg*, *Porphyromonas gingivalis*; *Fn*, *Fusobacterium nucleatum*; *Pi*, *Prevotella intermedia*, *Pn*, *Prevotella nigrescens*; *Aa, Aggregatibactor actinomycetemcomitans.*

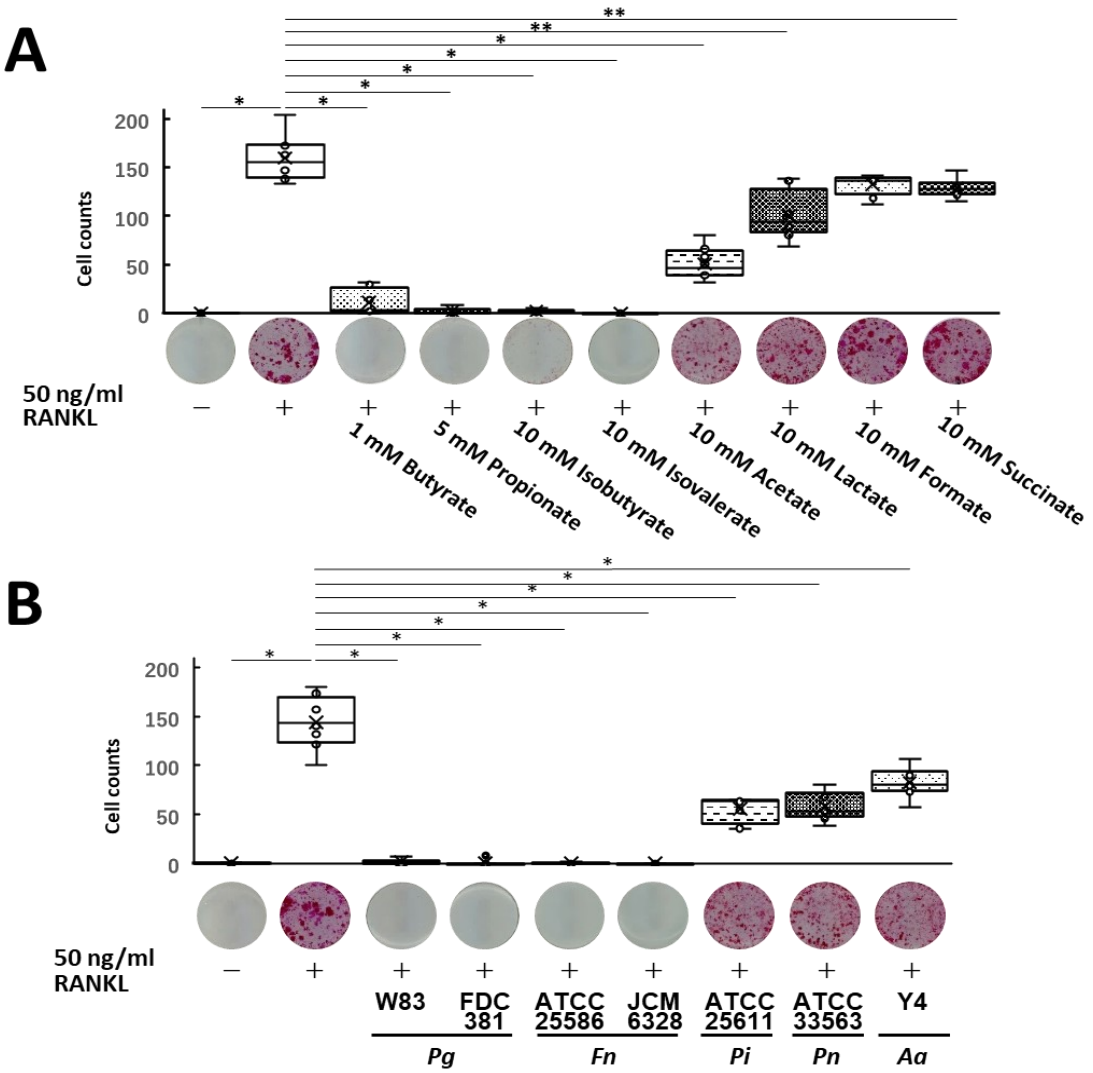

Fig. 2. SCFAs produced by oral bacteria suppress RANKL-induced osteoclast-like cell formation of RAW264.7 cells. (A) Murine macrophage-like RAW264.7 cells were treated for 4 days with 50 ng/ml RANKL in the presence or absence of the indicated concentrations of each SCFAs and subjected to TRAP staining. TRAP-positive multinuclear cells were counted as osteoclasts (n = 8; *, $P < 0.01$; **, $P < 0.05$). (B) Effects of SCFA-mixtures that mimic oral bacterial culture supernatants on RANKL-induced osteoclast formation. RAW264.7 cells were treated for 4 days with 50 ng/ml RANKL in the presence or absence of SCFA mixtures that mimic bacterial culture supernatants produced by oral bacteria and subjected to TRAP staining. TRAP-positive multinuclear cells were counted as osteoclasts (n = 8; *, $P < 0.01$). *Pg*, *Porphyromonas gingivalis*; *Fn*, *Fusobacterium nucleatum*; *Pi*, *Prevotella intermedia*, *Pn*, *Prevotella nigrescens*; *Aa*, *Aggregatibactor actinomycetemcomitans*.

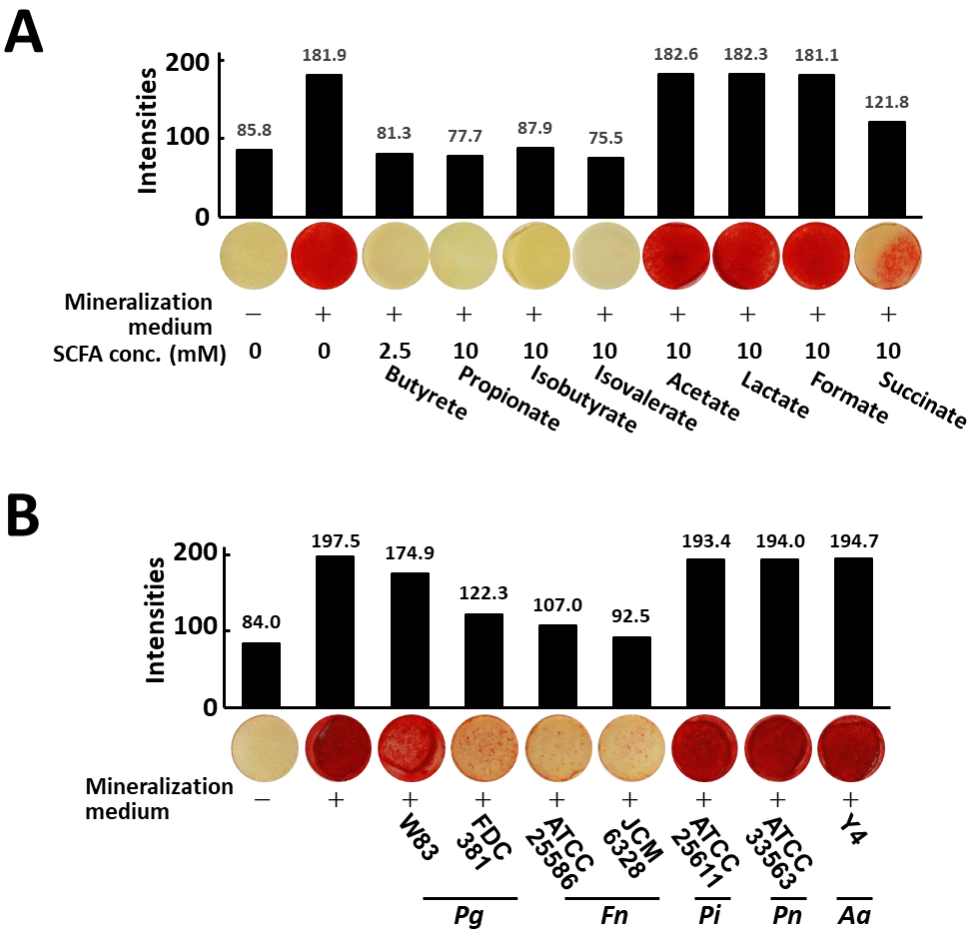

Fig. 3. SCFAs produced by oral bacteria augment mineralization medium-induced mineralization of osteoblastic MC3T3-E1 clone NDC10E1 cells. (A) Confluent murine osteoblast-like MC3T3-E1 clone NDC10E1 cells were cultured for 6 days in mineralization medium in the presence or absence of the indicated concentrations of each SCFAs, and the cells were then stained with Alizarin Red S. Red-intensities were measured using Fiji/Image J software. (B) Effects of SCFA-mixtures, which mimic bacterial culture supernatants, on mineralization-medium-indued MC3T3-E1 clone NDC10E1 cell mineralization. *Pg*, *Porphyromonas gingivalis*; *Fn*, *Fusobacterium nucleatum*; *Pi*, *Prevotella intermedia*, *Pn*, *Prevotella nigrescens*; *Aa*, *Aggregatibactor actinomycetemcomitans*.

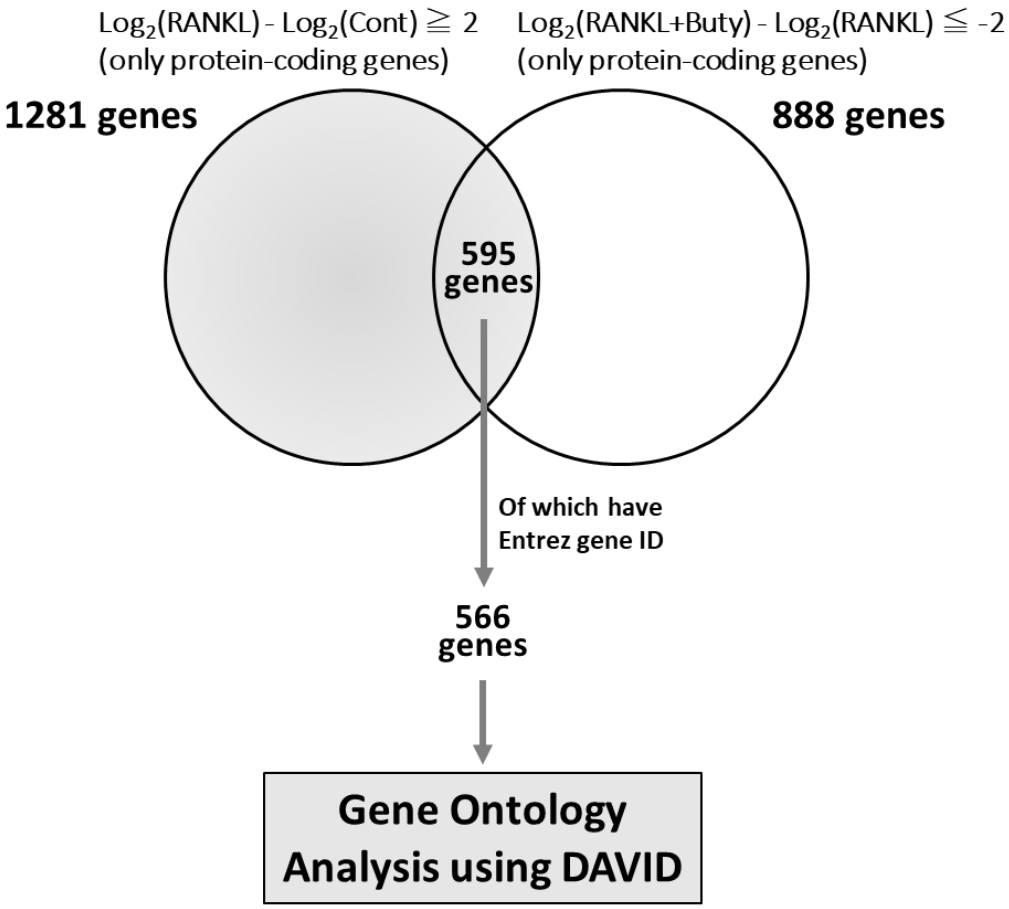

Fig. 4. RNA-sequencing analysis. RAW264.7 cells were treated for 48 h with (RANKL) or without (Cont) 50 ng/ml RANKL in the presence of 1 mM butyrate (RANKL+Buty). Total RNA was extracted from the cells, and RNA sequences were analyzed. TPM < 0.01 were omitted. A Venn diagram showing 595 RANKL-upregulated genes, which were downregulated by 1 mM butyrate treatment in the presence of 50 ng/ml RANKL. For GO enrichment analysis, 566 genes which have Entrez gene ID were used. RANKL + Buty, butyrate treatment in the presence of RANKL.

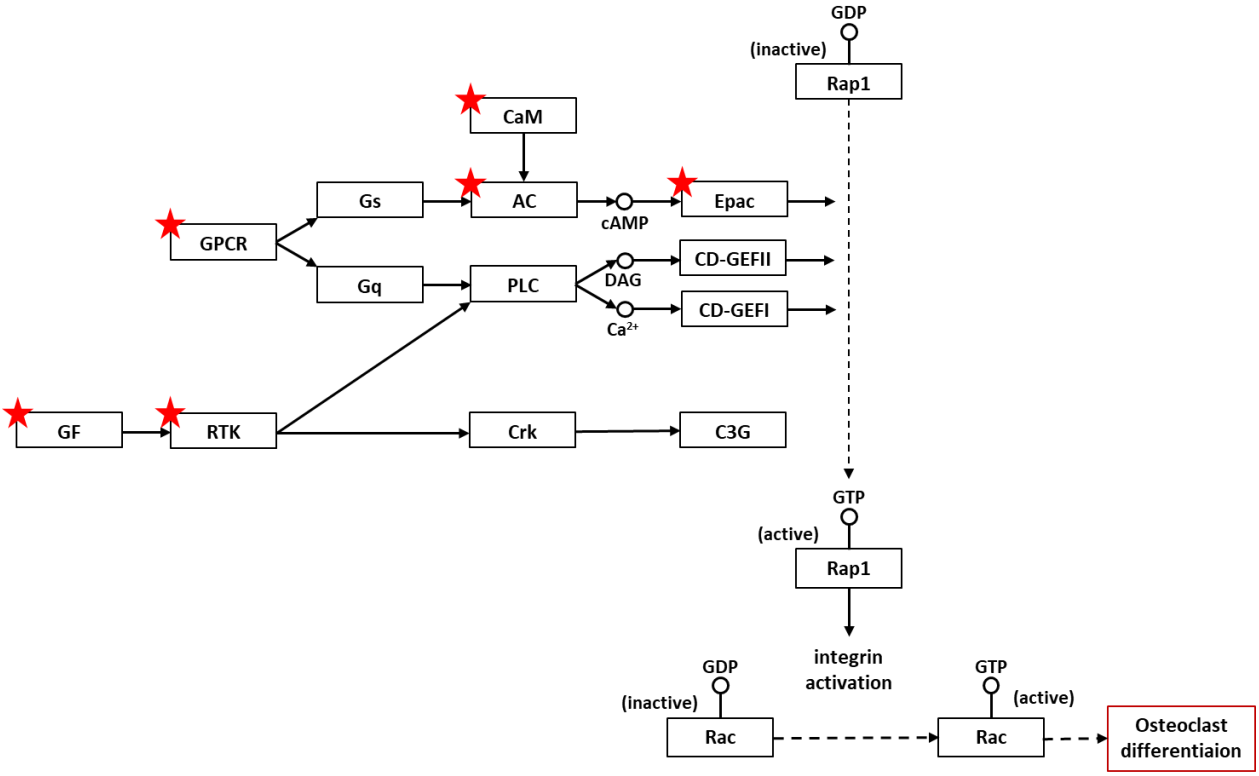

s

Fig. 5. A diagram of Rap1 signaling pathway on the KEGG pathway database. Selected 566 genes were applied to a GO-analysis using a DAVID program and the top 10 enriched pathways are listed in Table 3. The Rap1 signaling pathway is the highest ranked pathway which is reported to have relations to osteoclast differentiation. Presentative terms which include genes applied to GO-analysis were highlighted with red stars. AC, adenylate cyclase; CaM, calmodulin; cAMP, cyclic AMP; CD-GEF, calcium-and diacylglycerol-regulated guanine nucleotide exchange factor; DAG, diacylglycerol; Epac, cAMP-regulated guanine nucleotide exchange factor; GF, growth factor; GPCR, G protein-coupled receptor; PLC, phospholipase C; RTK, receptor tyrosine kinase. Genes highlighted with red stars are included in the genes which were selected for GO analysis.